# Self-consistent nonlocal feedback theory for electrocatalytic swimmers with heterogeneous surface chemical kinetics

Amir Nourhani,[1,*] Vincent H. Crespi,[1,2,3] and Paul E. Lammert[1]

[1]*Department of Physics, The Pennsylvania State University, University Park, Pennsylvania 16802, USA*

[2]*Department of Materials Science and Engineering, The Pennsylvania State University, University Park, Pennsylvania 16802, USA*

[3]*Department of Chemistry, The Pennsylvania State University, University Park, Pennsylvania 16802, USA*

(Received 13 January 2015; published 10 June 2015)

We present a self-consistent nonlocal feedback theory for the phoretic propulsion mechanisms of electrocatalytic micromotors or nanomotors. These swimmers, such as bimetallic platinum and gold rods catalyzing decomposition of hydrogen peroxide in aqueous solution, have received considerable theoretical attention. In contrast, the heterogeneous electrochemical processes with nonlocal feedback that are the actual "engines" of such motors are relatively neglected. We present a flexible approach to these processes using bias potential as a control parameter field and a locally-open-circuit reference state, carried through in detail for a spherical motor. While the phenomenological flavor makes meaningful contact with experiment easier, required inputs can also conceivably come from, e.g., Frumkin-Butler-Volmer kinetics. Previously obtained results are recovered in the weak-heterogeneity limit and improved small-basis approximations tailored to structural heterogeneity are presented. Under the assumption of weak inhomogeneity, a scaling form is deduced for motor speed as a function of fuel concentration and swimmer size. We argue that this form should be robust and demonstrate a good fit to experimental data.

DOI: 10.1103/PhysRevE.91.062303 PACS number(s): 82.45.−h

## I. INTRODUCTION

The development of electrocatalytic nanomotors over the past decade has opened a new area in colloid science focused on artificial self-propelling particles at the micro- and nanoscales [1–16]. These artificial swimmers can mimic the self-locomotion of small-Reynolds-number biological swimmers [17–21] by harvesting energy from their local environments to power rectilinear [22–27] or rotational [28–36] motion. Further development led to faster motors [24–26] and extra functionality [37–39]. An electrocatalytic motor consists of at least two metals decomposing a fuel asymmetrically. For example, hydrogen-peroxide-powered platinum and gold bimetallic motors produce hydrogen ions by oxidation of hydrogen peroxide mostly on the anodic platinum end and consume those same cations in cathodic reduction of hydrogen peroxide mostly on the gold end. The reaction-maintained nonequilibrium distribution of hydrogen ions gives rise to electrostatic body forces in the diffuse layer around the motor, which are responsible for the motor motion.

Given the reactive ion flux, time-tested methods of colloid science [40,41], with a few new twists [42–48], can be applied to compute the motor speed. Recently, we showed that for weak variation of potential over the spherical motor surface only the first Legendre coefficient of reactive cation flux contributes [48]. However, whence that reactive cation flux? While early work tended to simply take this ingredient as given [49,50], some later works [51–53] have attempted explicit incorporation of electrochemical kinetics. Beyond uncontrolled approximations, however, this is not as simple as it may appear at first glance. Self-consistency of such an approach is a nontrivial issue, as we shall see. The environmental conditions themselves, namely, concentration and electrostatic potential disturbances at the top of the diffuse layer, both influence local reaction rates and are influenced by reactions elsewhere on the surface.

In this paper we present a self-consistent nonlocal feedback (SCNLF) theory for electrocatalytic swimmers. We provide conceptually transparent self-consistent theory of heterogeneous surface electrochemistry with *nonlocal feedback* mediated by concentration and electric potential disturbances created at the top of the diffuse layer, the disturbances that are so central to the phoretic mechanism itself. The core formulation is given in operational terms, which means that the quantitative content can be connected directly to feasible, though perhaps challenging, experiments on the electrochemical characteristics of the metal surfaces constituting the motor. On the other hand, this machinery can also be straightforwardly connected to a Frumkin-Butler-Volmer (FBV) formulation. Even without parameter values or significant computation, this approach leads to a formula for motor speed as a function of fuel concentration and motor size that fits experimental data very well.

We work specifically with spherical swimmers that are compositionally axisymmetric. The symmetry restriction could be lifted fairly easily. Handling other swimmer shapes is more difficult. Shape enters in the Neumann-to-Dirichlet map (Sec. III) and in computing speed from reactive ion flux and potential (Sec. IV). The two important approximations we make from the very beginning are that the Debye screening length is small compared to the motor radius $a$ and that the Péclet number is small, allowing us to neglect the convective contribution to ionic currents. These approximations have a wide range of practical applicability. Since the time scale $t^* = a^2/D_r$ characterizes the time for a reactive cation of translational diffusivity $D_r$ to diffuse a distance comparable to the particle radius, the natural cation speed scale $U^\star = a/t^* = D_r/a$ is of order 1 mm/s for $a = 1$ $\mu$m. Motor speeds are typically two orders of magnitude smaller, so the Péclet number is comfortably

*nourhani@psu.edu

 

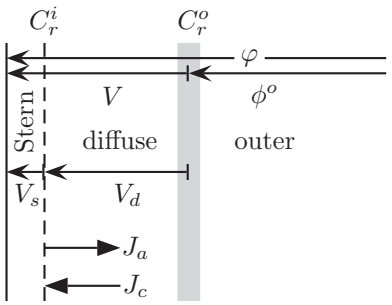


FIG. 1. The inner region, near the motor surface, is divided into the Stern layer and the diffuse layer. The electron electrochemical potential difference between infinity and the motor surface is decomposed into drops across these regions and layers.

small. This approximation decouples the analysis of the motor "engine" from calculation of the speed of the motor such that the fluid flow and swimmer movement can be considered side effects calculable *post hoc*. The Debye length, over which the electric potential is screened, is about 0.2 $\mu$m, which does not exceed 20% of the motor radius for typical swimmers, so the diffuse layer of screening ions around the motor is thin. Having discussed our approximations, we mention that extra inactive ions (salt) in the solution can be handled at almost no extra cost and the extension is practically important.

The chemical reactions involved in motor operation are introduced in schematic form in Sec. II. Also discussed there is the local thermodynamic equilibrium in the inner region consisting of Stern and diffuse layers (see Fig. 1) that serves to link conditions at the reaction plane to conditions in the outer region. Section III lays out the ionic kinetics in the outer region that mediates the nonlocal chemical feedback. Though this is a critical ingredient, the answer is simple and can be used as a black box for the rest of the SCNLF theory. Section IV gives a general expression for motor speed in terms of ion flux and interfacial potential drop. Although quantitative understanding of motor speed is the main motivation for everything done here, if motivation is granted it becomes somewhat peripheral. The treatment in this section is correspondingly brief. The heart of the paper is Sec. V, which sets forth the SCNLF theory in phenomenological form. Nonlocal feedback of surface reactive cation flux from concentration and potential disturbances on the top of the diffuse layer plays a prominent role. Our strategy for dealing with an inhomogeneous metal composition over the motor surface is based on using a heterogeneous surface bias field as a control parameter. We study the response to a small change of this field and set up an integration from a locally-open-circuit state (no net surface flux anywhere) to the actual state of uniform potential versus standard electrode. A very simple approximation appropriate to weak heterogeneity is treated in Sec. VI B and some more sophisticated ones in Sec. VI C, which attempt to take into account the most important components of compositional heterogeneity. Section VII shows how to obtain the ingredients of the self-consistent treatment from Frumkin-Butler-Volmer kinetics. This is applied to the weak-heterogeneity approximation to essentially recover a generalization of Sabass and Seifert's results [53]. Section VIII discusses a scaling form for swimmer speed as a function of fuel concentration and swimmer size. It is tested against data [27] from the literature and found to be consistent.

## II. LOCAL THERMODYNAMIC EQUILIBRIUM IN THE INNER REGION

Occurring at the surface of the swimmer is the anodic decomposition

$$m_a\mathcal{R} \to r + z_r e^- \tag{1}$$

of reactant $\mathcal{R}$, coupled with consumption of reactive cation $r$ (valence $z_r$) via the cathodic reaction

$$m_c\mathcal{R} + N\,r + N z_r e^- \to \mathcal{P}, \tag{2}$$

where $\mathcal{P}$ denotes product(s). Corresponding to these half reactions are position-dependent anodic $J_a$ and cathodic $J_c$ fluxes of the reactive cation, with a net position-dependent flux

$$J_r(\theta) = J_a(\theta) - J_c(\theta). \tag{3}$$

In the motivating case of bimetallic motors powered by the decomposition of hydrogen peroxide, $\mathcal{R}$ is $H_2O_2$ and the reactive cation $r$ is $H^+$. We now turn to a discussion of the environment in which these reactions occur.

A swimmer immersed in electrolyte develops a two-part entourage of ions. The Stern layer consists of ions adsorbed to the surface through specific interactions and is usually only a few angstroms thick. Beyond the Stern layer is the diffuse layer, a region of charge imbalance of dissolved ions that, in equilibrium, screens the residual charge of the swimmer plus Stern layer. The diffuse layer is well described by Gouy-Chapman theory, which treats the ions as point charges interacting via electrostatic forces. We refer to the diffuse layer and Stern layer as the inner region, which has a thickness of order Debye length $\lambda_D$. Outside the inner region is the outer region as shown in the diagram of Fig. 1. The inner-outer terminology is borrowed from the method of matched asymptotics at the thin diffuse layer, where it has a precise mathematical meaning. In this limit, aside from the chemical reactions at the surface, local thermodynamic equilibrium is attained across the inner region, since the equilibration time goes to zero. Thus, the position-dependent concentration $C_r^i$ of reactive cation at the reaction plane, which we take to coincide with the outer edge of the Stern layer, is related to the concentration $C_r^o$ at the inner-outer boundary by a Boltzmann factor containing the potential drop across the diffuse layer [54]:

$$C_r^i(\theta) = e^{-z_r V_d(\theta)/\phi^\star} C_r^o(\theta). \tag{4}$$

Here

$$\phi^\star := k_B T/e \tag{5}$$

is the thermal potential, $k_B$ is the Boltzmann constant, $e$ is the magnitude of the electron charge, $z_r$ is the charge of species $r$, and $V_d$ is the potential at the slip plane (assumed to approximately coincide with the reaction plane) relative to the top of the diffuse layer, i.e., essentially the $\zeta$ potential (zeta potential).

The condition of local equilibrium also determines the partitioning of the potential drop $V$ across the inner region

into potential drops across the Stern layer $V_s$ and diffuse layer $V_d$ as

$$V = V_s + V_d. \tag{6}$$

Alternatively,

$$V = \varphi - \phi^o \tag{7}$$

is the difference between the potential $\varphi$ just on the metal surface (surface bias) and the potential $\phi^o$ at the inner-outer boundary. All of our potentials are interpreted in an operational sense as potential versus standard electrode and are therefore really (up to a factor $-e$) electrochemical potentials for electrons. An important consequence of this, and the reason for the convention, is that $\varphi$ is uniform over the entire surface under realistic conditions, irrespective of composition variations, since the motor is assumed strongly electrically connected.

The anodic and cathodic fluxes (3) depend on *local* chemical and electronic surface characteristics in conjunction with the concentration at the reaction plane and the voltage drop across the Stern layer $\{C_r^i(\theta), V_s(\theta)\}$. Due to the local thermodynamic equilibrium, $V_s(\theta)$ and $C_r^i(\theta)$ are determined by $V(\theta)$ and the concentrations $C_\beta^o(\theta)$'s of all ionic species at the inner-outer boundary. This latter parametrization sounds much more complicated since there may be many ionic species. The reason we need concentrations of chemically inert species, at least in principle, is that they may influence adsorption in the Stern layer. The reason this parametrization is preferable becomes clear in Sec. V.

## III. FROM ION FLUX TO CONCENTRATION AND POTENTIAL DISTURBANCE

In this section we derive a relation between the ion flux and the potential and concentration disturbances on the boundary of the outer layer via a Neumann-to-Dirichlet map. That relation holds for arbitrary swimmer shape, but for a sphere we can write down an explicit and simple expression.

We start with the equation

$$\boldsymbol{J}_\beta = -D_\beta(\nabla C_\beta^o + z_\beta C_\beta^o \nabla\phi^o/\phi^\star) + C_\beta^o \boldsymbol{U}^o \tag{8}$$

for the flux of ionic species $\beta$ in the outer region. Note that, in this section, the fields $C_\beta^o$ and $\phi^o$ are defined throughout the outer region. Elsewhere, we use the same notation to refer to just the inner-outer boundary. Dropping the bulk velocity term since the Péclet number is small (as discussed in the Introduction) and linearizing yields

$$-D_\beta^{-1}\boldsymbol{J}_\beta = \nabla\delta C_\beta^o + z_\beta C_\beta^\infty \nabla\phi^o/\phi^\star, \tag{9}$$

where $\delta C_\beta^o = C_\beta^o - C_\beta^\infty$ is the deviation from bulk concentration. At steady state, $\nabla\cdot\boldsymbol{J}_\beta = 0$ and by electroneutrality

$$\sum_\beta z_\beta\, \delta C_\beta^o = 0 \tag{10}$$

and $\phi^o$ obeys the Laplace equation. Therefore, so does $\delta C_\beta^o$, for each $\beta$:

$$\nabla^2\phi^o = 0, \quad \nabla^2\delta C_\beta^o = 0. \tag{11}$$

Multiply Eq. (9) by $z_\beta$, take the normal component at the boundary $\partial\Omega^o$ of the outer region, sum over $\beta$, and apply the electroneutrality condition (10) to obtain

$$a\hat{n}\cdot\nabla\phi^o|_{\partial\Omega^o} = -\frac{z_r\phi^\star}{2J^\star}J_r. \tag{12}$$

Here $\hat{n}$ is normal to the surface at the boundary $\partial\Omega^o$ and we have introduced a characteristic ion flux scale

$$J^\star := \frac{D_r I}{a}, \tag{13}$$

defined in terms of the usual ionic strength

$$I = \frac{1}{2}\sum_\beta z_\beta^2 C_\beta^\infty. \tag{14}$$

Correspondingly, the boundary condition on the normal derivative of the concentration of species $\beta$ is

$$a\hat{n}\cdot\nabla\delta C_\beta^o|_{\partial\Omega} = -Y_\beta\frac{J_r}{J^\star}, \tag{15}$$

where

$$Y_\beta := I\delta_{\beta r} - \tfrac{1}{2}z_r z_\beta C_\beta^\infty, \tag{16}$$

where $\delta_{\beta r}$ is the Kronecker delta. In particular,

$$Y_r = I - \tfrac{1}{2}z_r^2 C_r^\infty \tag{17}$$

is a reduced ionic strength with the contribution of reactive ions subtracted out.

The concentration deviations $\delta C_\beta^o$, along with $\phi^o$, satisfy the Laplace equation (11) in the outer region $\Omega$ and tend to zero at infinity. If $f$ is such a function (harmonic, decaying to zero), then it is determined uniquely by boundary conditions of either Dirichlet type, specifying $f|_{\partial\Omega}$, or Neumann type, specifying $\hat{n}\cdot\nabla f|_{\partial\Omega}$ (among others). We define the Neumann-to-Dirichlet map

$$\mathcal{L}g = f|_{\partial\Omega}, \tag{18}$$

where $\nabla^2 f = 0$ on $\Omega$, $f(x) \overset{|x|\to\infty}{\longrightarrow} 0$, and $\hat{n}\cdot\nabla f|_{\partial\Omega} = g$ as an operator converting the Neumann boundary data to the Dirichlet boundary data. Applied to our problem,

$$\left.\frac{\phi^o}{\phi^\star}\right|_{\partial\Omega^o} = \frac{z_r}{2}\mathcal{L}\frac{J_r}{J^\star}, \tag{19a}$$

$$\left.\delta C_\beta^o\right|_{\partial\Omega^o} = Y_\beta\mathcal{L}\frac{J_r}{J^\star}. \tag{19b}$$

In the literature, such maps are often used the other way around and hence are called Dirichlet-to-Neumann maps [55] or even Neumann operators [56]; more generally, boundary-changing operators are referred to as Poincaré-Steklov maps [57]. In the rest of this paper we are interested in $\phi^o$ and $\delta C_\beta^o$ only at the boundary of the outer region; to lighten the notational load, $|_{\partial\Omega^o}$ will therefore not be written.

So far, the development has been independent of swimmer shape. Now we specialize to the case of particular interest, a compositionally axisymmetric spherical swimmer, in order to obtain explicit expressions, using the classical theory of the Laplace equation in spherical coordinates [58,59]. Since Legendre expansions will occur frequently, we introduce the notation $(\!|\cdot|\!)_m$ for $m$th expansion coefficients. Thus, the

Legendre expansion of an axisymmetric function $f(\theta)$ on the surface of the sphere reads

$$f(\theta) = \sum_{m=0}^{\infty} (\!|f|\!)_m P_m(\cos\theta), \tag{20}$$

where $P_m$ is the Legendre polynomial of degree $m$. With this notation [48],

$$(\!|\mathcal{L}f|\!)_m = \frac{1}{m+1}(\!|f|\!)_m. \tag{21}$$

This is straightforwardly verified, using the fact that axisymmetric exterior solutions to the Laplace equation tending to zero at infinity are linear combinations of $\{r^{-(m+1)}P_m(\cos\theta)|m \geqslant 0\}$. Note that $\mathcal{L}$ has a smoothing effect, since higher Legendre expansion coefficients are more strongly damped.

## IV. MOTOR SPEED

Anderson and Prieve [60] showed that for a spherical particle driven by any phoretic mechanism over a thin interfacial layer, the particle velocity is equal to the surface average of minus the slip velocity. In the case of a symmetric electrolyte ($|z_\beta| = z$ for all $\beta$), the local slip velocity is given by the Dukhin-Derjaguin formula [51,61]

$$\boldsymbol{U}_{\text{slip}} = 4\,\text{Pe}\frac{U^\star}{z^2}\left[z^2\frac{V_d}{4\phi^\star}\frac{\partial_\theta\phi^o}{\phi^\star} - \left(\ln\cosh\frac{zV_d}{4\phi^\star}\right)\frac{\partial_\theta C_+^o}{C_+^o}\right]\hat{e}_\theta. \tag{22}$$

Here

$$\text{Pe} = \frac{\epsilon(\phi^\star)^2}{\eta D_r} \tag{23}$$

is identified as a Péclet number appropriate to our problem and is about 0.05 at room temperature if the reactive cation is $H^+$,

$$U^\star := \frac{D_r}{a} \tag{24}$$

is the characteristic velocity scale mentioned in the Introduction, $V_d(\theta)$, we recall, is the potential drop across the diffuse layer, and $C_+^o$ is the total concentration of positive species. Restriction of the electrolyte composition occurs only in this section. If it is not symmetric, the second term inside large square brackets in (22) will be incorrect and there is no explicit expression available. However, if $V_d \ll \phi^\star$ (weak $\zeta$ potential), then that term can be dropped anyway and the electrolyte composition again becomes unimportant.

Using (19) and a little algebra, we find

$$\frac{\partial_\theta C_+^o}{zC_+^\infty} = \frac{\partial_\theta\phi^o}{\phi^\star}, \tag{25}$$

which in the linear regime recasts the slip velocity (22) into

$$\boldsymbol{U}_{\text{slip}}(\theta) = 4\,\text{Pe}\,\frac{U^\star}{z}\,\ln\left(1+\tanh\frac{zV_d}{4\phi^\star}\right)\frac{\partial_\theta\phi^o}{\phi^\star}\hat{e}_\theta. \tag{26}$$

It is remarkable that, expressed purely in terms of $\phi^o$, the slip velocity turns out to be independent of the electrolytic composition.

Computing the average of (26) for an axisymmetric sphere yields the motor velocity

$$\boldsymbol{U} = -\overline{\boldsymbol{U}_{\text{slip}}} = \hat{e}_z\text{Pe}\frac{U^\star}{2z}\int_0^\pi \Psi(\theta)\frac{\partial_\theta\phi^o}{\phi^\star}\sin^2\theta\,d\theta, \tag{27}$$

where $\hat{e}_z$ is the direction of the symmetric axis and

$$\Psi := 4\ln\left(1+\tanh\frac{zV_d}{4\phi^\star}\right). \tag{28}$$

Rewritten in terms of Legendre coefficients (20) of $\Psi$ and $J_r$, we obtain a general expression for swimmer speed; Eq. (27) becomes

$$\boldsymbol{U} = \hat{e}_z\text{Pe}\frac{U^\star}{2}\sum_{n=1}^{\infty}\frac{(\!|J_r|\!)_n}{J^\star}\frac{n}{2n+1}\left(\frac{(\!|\Psi|\!)_{n-1}}{2n-1} - \frac{(\!|\Psi|\!)_{n+1}}{2n+3}\right). \tag{29}$$

Equation (29) clearly shows the importance of $J_r$ and $V_d$ to the motor speed. It is plausible that motor operation will not greatly perturb $V_d$, so it can be approximated [48] by a value for the inert, fuel-deprived, swimmer. In that case, $J_r$ is the critical ingredient. Calculating it, on the basis of a self-consistent theory for the mixed potential of the motor as a whole, is the main goal of the rest of this paper. Here $V_d$ plays a subordinate role in that endeavor, in that it does not appear at all in the phenomenological version. If the above-mentioned approximation is not adequate, then in order to find $V_d$ it is necessary to use Eq. (57b) as well.

## V. SELF-CONSISTENT NONLOCAL FEEDBACK THEORY

This section is the conceptual core of the paper. We expose and discuss the self-consistency problem among the reactive cation flux $J_r$ on the top of the Stern layer, $C_r^o$, and $\phi^o$ at the top of the diffuse layer that arises when chemical kinetics is taken into account. Explicit Frumkin-Butler-Volmer kinetics will be treated in Sec. VII, but here we use a general operational description that can be more easily related to experiments and is also reducible to FBV parametrization.

Equation (19) showed that the disturbances of reactive cation concentration and potential at the inner-outer boundary are simply related to the cation flux on the top of the Stern layer via the nonlocal Neumann-to-Dirichlet map $\mathcal{L}$. The nonlocality implies chemical kinetics on different regions of the reaction surface communicate through their sensitivity to the position-dependent pair $\{\delta C_r^o, \phi^o\}$. The variations of $\delta C_\beta^o$ depend on the variation of $\delta C_r^o$ through the constraint

$$C_\beta^o = C_\beta^\infty + (Y_\beta/Y_r)\delta C_r^o \tag{30}$$

imposed by Eq. (19b). On the other hand, the chemical kinetics itself, which determines the reactive cation flux $J_r$ on the top of the Stern layer, is local. These interlocking dependences give rise to the self-consistency loop, illustrated in Fig. 2. Since $J_r$ and the pair $\{\delta C_r^o, \phi^o\}$ are inside the loop here, attempting to dictate the value of one of them risks running afoul of the self-consistency. Instead, we use the surface bias field $\varphi$ as a control parameter (see Fig. 1). We will derive local relations for the changes of $J_r$, $\delta C_r^o$, and $\phi^o$ induced by a small local change of $\varphi$. These can then be integrated from some initial position-dependent value $\varphi(\theta)$ to the final uniform value of

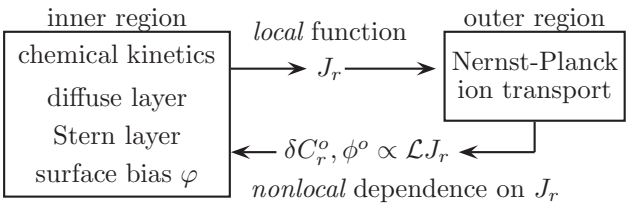


FIG. 2. Self-consistency loop. The electrochemical kinetics in the inner region is affected by ion transport in the outer region in a way that leads to nonlocal feedback.

$\varphi$ at which the net reactive cation flux from the swimmer is zero. A very useful initial condition is one for which we know the values of $J_r$, $\delta C_r^o$, and $\phi^o$ without explicitly solving the self-consistency problem from some random initial condition. The hypothetical locally-open-circuit state provides us with such an initial condition, so we turn to an explication of this concept and mixed potential.

First consider the system in Fig. 3 containing a reference standard (e.g., hydrogen) electrode and two electrodes labeled (with a little foresight) "anode" and "cathode." With the switch $\mathcal{S}$ open, the current $i_a$ into the anode vanishes when $V_a$, the electrochemical potential of the anode with respect to the reference standard electrode, is set to $V_{a,\mathrm{mxd}}$, the mixed potential (denoted by the subscript mxd), which depends on the composition of the electrode. Similarly, $i_c$ vanishes when we set the cathode potential to its mixed potential $V_c = V_{c,\mathrm{mxd}}$. Zero current on an electrode does not mean that there is no reaction on the electrode surface, only that the anodic and cathodic reactions on it are balanced. If we increase $V_a$ a little, $i_a$ will increase, and if we decrease $V_c$ a little, $i_c$ will increase. At some intermediate common potential $V_a = V_c = V$ satisfying $V_{a,\mathrm{mxd}} < V < V_{c,\mathrm{mxd}}$, the currents become equal $i_a = i_c \neq 0$. At that point, current no longer flows through the standard electrode; if $\mathcal{S}$ is closed, the current will flow directly from the cathode to the anode. The common final voltage is the mixed potential of the composite anode-cathode system and the inequality $V_{a,\mathrm{mxd}} < V_{c,\mathrm{mxd}}$ determines which electrode is the anode and which is the cathode. Essentially this reasoning was used by Wang *et al.* [62] to rationalize the direction of motion of bimetallic motors with anode forward for a variety of metal pairs. Now we will combine it with the self-consistency problem to get quantitative results.

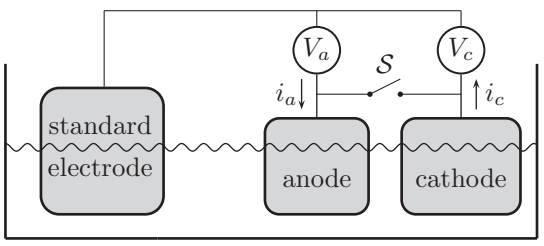


FIG. 3. The mixed potential of an individual electrode corresponds to a steady state in which the net current through it is zero. The collective mixed potential of the anode-cathode combination, which is intermediate between the individual mixed potentials, involves a current between them, but none through the standard electrode.

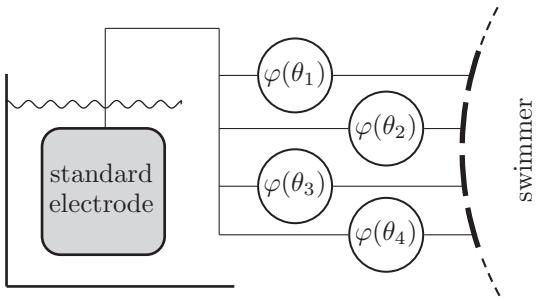


FIG. 4. Imaginary subdivision of the swimmer surface into a collection of isolated patches connected to a standard electrode through individual voltage sources.

With this introduction, let us return to the problem of the swimmer. We divide the compositionally heterogeneous surface of the swimmer into small patches, each with uniform composition. As depicted in Fig. 4, now imagine a hypothetical scenario where these patches are electrically isolated from each other and each is connected to a standard electrode through its own voltage source. This situation is much like the preceding anode-cathode system in Fig. 3, just with more electrodes. The electrically isolated patch at $\theta$ has its own mixed potential $\varphi_{\mathrm{mxd}}(\theta)$ depending on the patch's composition. With the bias of each patch adjusted to its own proper mixed potential, the reactive ion flux $J_r(\theta)$ is everywhere zero and so too are $\delta C_r^o(\theta)$ and $\phi^o(\theta)$. This situation provides a very convenient (although fictitious) initial condition from which we can make the following adjustment to achieve the experimentally relevant conditions: When the bias voltages are brought to a common value at which the net ion flux from the swimmer is zero, the imaginary apparatus and electrical isolation can be removed without effect. That common value is the actual mixed potential of the swimmer as a whole, which of course does not actually have either the voltage sources or electrical isolation. The main task is to see how such a final uniform bias voltage can be determined.

With the idea of surface bias $\varphi$ as a theoretical control field in hand, we return to the self-consistency problem $J_r \overset{\varphi}{\leftrightarrow} \{\delta C_r^o, V\}$ in Fig. 2. Rather than tackling it all at once, we ask how the solution changes if the surface bias control field $\varphi(\theta)$ is changed a little bit. We immediately have

$$dJ_r = \left(\frac{\partial J_r}{\partial V}\right)_{C_r^o} dV + \left(\frac{\partial J_r}{\partial C_r^o}\right)_V dC_r^o, \tag{31}$$

as well as [see Eq. (19)]

$$\begin{aligned} dV &= d\varphi - d\phi^o, \\ \frac{d\phi^o}{\phi^\star} &= \frac{z_r}{2}\mathcal{L}\frac{dJ_r}{J^\star}, \\ \frac{dC_r^o}{Y_r} &= \mathcal{L}\frac{dJ_r}{J^\star}. \end{aligned} \tag{32}$$

A little algebra puts the preceding system of equations into a form that allows sequential calculation of all the increments given $d\varphi$. First,

$$dJ_r = \left[1 + \frac{\Gamma}{J^\star}\mathcal{L}\right]^{-1} G\, d\varphi, \tag{33}$$

with

$$G = \left(\frac{\partial J_r}{\partial V}\right)_{C_r^o} \tag{34}$$

and

$$\Gamma := \frac{1}{2} z_r \phi^\star G - Y_r \left(\frac{\partial J_r}{\partial C_r^o}\right)_V, \tag{35}$$

where $G$ and $\Gamma$ are local current-response characteristics of the surface that mediate the relation $J_r \overset{\varphi}{\leftrightarrow} \{\delta C_r^o, \phi^o\}$ and $(\Gamma/J^\star)\mathcal{L}$ in Eq. (33) represents the nonlocal feedback. Here $G$ is essentially the differential interfacial conductivity, the derivative being taken with all ionic concentrations fixed. Similarly, the second term in $\Gamma$ measures the response of the flux to a change of the concentrations while the constraint (30) is maintained. With explicit Frumkin-Butler-Volmer kinetics in Sec. VII, this will be clearer. Here $G$ and $\Gamma$ are local characteristics in that they depend upon the conditions $\{\delta C_r^o(\theta), V(\theta)\}$ and thus vary with position and also in that they do not depend on the overall geometry of the swimmer. It was for that reason that $J^\star$ was factored out in (33): It is the only place where the size of the swimmer enters the formalism. We emphasize that both $G$ and $\Gamma$ are operationally meaningful. It is possible to perform measurements corresponding to the derivatives in Eqs. (34) and (35).

Given these current-response characteristics, we can integrate Eqs. (32) and (33) along a path in $\varphi(\theta)$ space to obtain a path in $\{C_r^o(\theta), \phi^o(\theta), J_r(\theta)\}$ space. We recall that all the ionic concentrations vary according to the constraint (30) with deviations from bulk values all locally proportional to $\delta C_r^o(\theta)$, so the latter serves to coordinatize the concentration variations. Starting, then, from the locally-open-circuit state $\varphi^{(0)}(\theta) = \varphi_{\rm mxd}(\theta)$ implying zero local flux $J_r(\theta) = 0$, we integrate to a state of uniform bias with zero net flux $\int_S J_r dS = 0$, but nonzero local flux $J_r(\theta) \neq 0$. This presents two problems: determining the current-response characteristics $G$ and $\Gamma$ and finding manageable approximations to handle the spatial inhomogeneities. As $G$ and $\Gamma$ have relatively straightforward operational meaning, direct electrochemical laboratory measurement is possible. For each metal composing the motor, a sequence of measurements is to be done with an electrode of that composition, varying the potential versus standard electrode and the bulk concentrations of the various ionic species. Given the complete functional dependence of $G$ and $\Gamma$ for the metals comprising the motor, exact integration is possible, though it must be done numerically. In Sec. VII we treat the current-response characteristics in the framework of Frumkin-Butler-Volmer kinetics.

## VI. APPROXIMATION SCHEMES

### A. Generalities

Although our notation does not make it explicit, the parameters $G$ and $\Gamma$ potentially depend upon the environmental conditions $\{C_r^o(\theta), \phi^o(\theta)\}$ as well as position on the surface. Integration of Eqs. (32) and (33) leads to a path in $\{C_r^o(\theta), \phi^o(\theta)\}$ space, which, for purposes of convenient discussion, we temporarily parametrize the path by a variable $s$. At each value of $s$, we have functions $G_s$ and $\Gamma_s$ over the surface. There are then two intuitive approximations. First, we might neglect variation of $G_s$ and $\Gamma_s$ along the integration contour, that is to say, their $s$ dependence. This is reasonably described as treating $G$ and $\Gamma$ as constant (functions of $\theta$). The second approximation is to neglect variation of $G_s$ and $\Gamma_s$ with respect to position on the surface. That is, we treat them as uniform (functions of $s$). Realistically, if uniformity is a reasonable approximation, the path in $\{C_r^o(\theta), \phi^o(\theta)\}$ is probably very short, so constancy will also be a reasonable assumption. Considering the current characteristics as constant has a dramatic mathematical effect in that Eqs. (32) and (33) can be integrated in a single step, thus ceasing to be genuine differential equations. However, these equations are equations for fields $J_r$, $\phi^o$, and $C_r^o$ with infinitely many degrees of freedom. Cutting them down is in principle independent of what we do with the current characteristics, but it does not make much sense to treat the fields more coarsely.

The calculationally simplest situation is that of uniform and constant $G$ and $\Gamma$, which is applicable if the metals comprising the motor are sufficiently similar. This is pursued in Sec. VI B. In Sec. VI C we attempt to take into account the most important variation across the surface by working in a two-dimensional space of functions on the sphere.

### B. Weak heterogeneity

For sufficiently weak heterogeneity, we take $\Gamma$ and $G$ to be uniform and constant, equal to nominal or average values written simply as $\Gamma$ and $G$. Such a drastic simplification of the parameters means we can treat the fields with no approximation. We can integrate Eq. (33) from an initial surface bias $\varphi^{(0)}(\theta) = \varphi_{\rm mxd}(\theta)$ to a final uniform value (to be checked in a moment)

$$\overline{\varphi_{\rm mxd}} \equiv (\!|\varphi_{\rm mxd}|\!)_0 \tag{36}$$

in a single step. The result, expressed in terms of Legendre expansion coefficients (20), is

$$\frac{(\!|J_r|\!)_m}{J^\star} = -\left(J^\star + \frac{\Gamma}{m+1}\right)^{-1} G (\!|\varphi_{\rm mxd} - \overline{\varphi_{\rm mxd}}|\!)_m. \tag{37}$$

This gives $(\!|J|\!)_0 = 0$, verifying that $\varphi = \overline{\varphi_{\rm mxd}}$ really is the correct uniform bias.

This approximation can be thought of as linearizing in the inhomogeneity. The variation of local mixed potential across the surface is first order in inhomogeneity, so everything else may be taken to zeroth order. If we then use this flux to compute motor speed (29), it is appropriate to use just $(\!|J|\!)_1$ coupled with the nominal $\zeta$ potential

$$\zeta = (\!|V_d|\!)_0 \simeq \frac{\phi^\star}{z} (\!|\Psi|\!)_0. \tag{38}$$

This yields

$$U \simeq \frac{z\epsilon\phi^\star \zeta G}{6\eta D_r I} \frac{(\!|\overline{\varphi_{\rm mxd}} - \varphi_{\rm mxd}|\!)_1}{1 + \Gamma/2J^\star}, \tag{39}$$

which reveals a crossover with increasing swimmer size ($a \propto 1/J^\star$) from $U \propto$ const at small $a$ to $U \propto 1/a$ at large $a$. We return to this observation in Sec. VIII.

### C. Small-basis approximations

The next level of approximation takes into account heterogeneity of the current-response characteristics $\Gamma$ and $G$. The approximations used are two-dimensional function space and meant to capture both the averages and the predominant shape of the heterogeneity of $\Gamma$ and $G$. In order to do that, we need a clearly defined approximation space $\mathcal{H}$ and an unambiguous way to approximate functions by elements of $\mathcal{H}$. Not only the parameters, but also the fields will be subjected to the same spatial approximation. For that, we use the following inner product on square-integrable axisymmetric functions on the sphere:

$$\langle f|g\rangle := \frac{1}{2}\int_0^\pi f(\theta)g(\theta)\sin\theta\, d\theta. \tag{40}$$

The normalization chosen here has no effect on the ultimate results, but is convenient since it makes the constant function 1 into a unit vector in our function space. Given an orthonormal basis $\{\hat\psi_0(\theta),\hat\psi_1(\theta)\}$ for the two-dimensional approximation space $\mathcal{H}$, functions are projected into $\mathcal{H}$ to become two-dimensional column vectors according to

$$f \mapsto \begin{bmatrix}\langle\psi_0|f\rangle\\ \langle\psi_1|f\rangle\end{bmatrix}. \tag{41}$$

Operators such as the Neumann-to-Dirichlet map $\mathcal{L}$ are converted into $2\times 2$ matrices:

$$A \mapsto [A] = \begin{bmatrix}A_{00} & A_{01}\\ A_{10} & A_{11}\end{bmatrix}, \quad A_{ij} = \langle\psi_i|A\psi_j\rangle. \tag{42}$$

We shall consider two different approximation spaces. For each, the constant $\hat\psi^0 = 1$ is one basis element. The second will have different signs on the two ends of the swimmer and aims to capture the most important kind of variation along the surface. In view of the importance of the first Legendre coefficient of $J_r$ for a uniform-$\zeta$ sphere, one reasonable choice is

$$\hat\psi_0^L(\theta) = 1, \quad \hat\psi_1^L(\theta) = \sqrt{3}\cos\theta \quad \text{(Legendre)}.$$

If, on the other hand, we consider swimmers that have homogeneous composition across each of the northern and southern hemispheres, this basis seems fitting:

$$\hat\psi_0^H(\theta) = 1, \quad \hat\psi_1^H(\theta) = \mathbf{1}[\theta < \pi/2] - \mathbf{1}[\theta \geqslant \pi/2] \quad \text{(Haar)}.$$

Before putting these to work, we develop a little further the common matrix algebra that applies to any basis with $\hat\psi_0 = 1$. Rewriting the fundamental equation (33) in matrix form yields

$$\left\{\mathcal{I} + \frac{1}{J^\star}[\Gamma][\mathcal{L}]\right\}\begin{bmatrix}\langle 1|dJ_r\rangle\\ \langle\hat\psi_1|dJ_r\rangle\end{bmatrix} = [G]\begin{bmatrix}\langle 1|d\varphi\rangle\\ \langle\hat\psi_1|d\varphi\rangle\end{bmatrix}, \tag{43}$$

where $\mathcal{I}$ is the identity matrix. A potentially confusing point is that $\Gamma$ and $G$ appear here as matrices. Although they are functions, their role in the equation is rather as multiplication operators, therefore we compute their matrix elements as in (42), where, for example, $G\hat\psi_j$ is understood simply as the multiplication of the two functions such that $G_{ij} = \frac{1}{2}\int_0^\pi \hat\psi_i G\hat\psi_j \sin\theta\, d\theta$.

Assuming that there is no net current ($\overline{J} = 0$) out of the motor in the initial state and we wish to maintain that throughout the integration, the condition

$$\langle 1|dJ_r\rangle = \overline{dJ}_r = 0 \tag{44}$$

is imposed. Using this and $\mathcal{L}_{01} = (\!|\hat\psi_1|\!)_0 = 0$, Eq. (43) can be reduced to

$$\langle\hat\psi_1|dJ_r\rangle = \frac{J^\star\det[G]}{G_{00}(J^\star + \Gamma_{11}\mathcal{L}_{11}) - G_{10}\Gamma_{01}\mathcal{L}_{11}}\langle\hat\psi_1|d\varphi\rangle, \tag{45}$$

which determines $\langle\hat\psi_1|dJ_r\rangle$, and

$$\overline{d\varphi} = \frac{-G_{01}(J^\star + \Gamma_{11}\mathcal{L}_{11}) + G_{11}\Gamma_{01}\mathcal{L}_{11}}{J^\star\det[G]}\langle\hat\psi_1|dJ_r\rangle, \tag{46}$$

which then determines the change $\overline{d\varphi}$ of the average bias.

In the case that it is possible to neglect variation of the response characteristics $\Gamma$ and $G$ along the integration, the differential equations (45) and (46) can be reduced to algebraic equations by the substitution

$$\begin{bmatrix}\overline{d\varphi}\\ \langle\hat\psi_1|d\varphi\rangle\end{bmatrix} \mapsto \begin{bmatrix}\varphi - \overline{\varphi_{\mathrm{mxd}}}\\ -\langle\hat\psi_1|\varphi_{\mathrm{mxd}}\rangle\end{bmatrix}, \tag{47}$$

where $\varphi$ is the final uniform bias of the motor.

Now we specialize these to our chosen bases, beginning with the Legendre basis. Here $\mathcal{L}$ is diagonal, so it is easy to deal with. For the operator of multiplication by an arbitrary function $f(\theta)$, the matrix is

$$[f] = \begin{bmatrix}(\!|f|\!)_0 & \frac{1}{\sqrt{3}}(\!|f|\!)_1\\ \frac{1}{\sqrt{3}}(\!|f|\!)_1 & \frac{2}{5}(\!|f|\!)_2 + (\!|f|\!)_0\end{bmatrix}. \tag{48}$$

In order to maintain a situation where only knowledge of the first two Legendre expansion coefficients is required, we drop the $(\!|f|\!)_2$ terms in the following. Under that (additional) approximation $\det[G] = \overline{G}^2 - \frac{1}{3}(\!|G|\!)_1^2$, using $\langle\hat\psi_1^L|\mathcal{L}\hat\psi_1^L\rangle = \frac{1}{2}$, $\langle\hat\psi_1^L|f(\theta)\rangle = \frac{2}{3\sqrt{3}}(\!|f|\!)_1$, and Eq. (45), the reactive cation flux is

$$\frac{(\!|J_r|\!)_1}{J^\star} = \frac{-\left[\overline{G}^2 - \frac{1}{3}(\!|G|\!)_1^2\right]}{\overline{G}\left[J^\star + \frac{1}{2}\overline{\Gamma}\right] - \frac{1}{6}(\!|G|\!)_1(\!|\Gamma|\!)_1}(\!|\varphi_{\mathrm{mxd}}|\!)_1 \tag{49}$$

and the deviation of the composite mixed potential from the area average is

$$\varphi - \overline{\varphi_{\mathrm{mxd}}} = \frac{1}{3}\left(\frac{(\!|G|\!)_1\left[J^\star + \frac{1}{2}\overline{\Gamma}\right] - \frac{1}{2}\overline{G}(\!|\Gamma|\!)_1}{\overline{G}\left[J^\star + \frac{1}{2}\overline{\Gamma}\right] - \frac{1}{6}(\!|G|\!)_1(\!|\Gamma|\!)_1}\right)(\!|\varphi_{\mathrm{mxd}}|\!)_1. \tag{50}$$

Note that if we throw away $(\!|G|\!)_1$ and $(\!|\Gamma|\!)_1$, (49) reduces to our weak-heterogeneity approximation (37) and the shift of the composite mixed potential vanishes.

The corresponding computations in the Haar basis have a few differences. A nice feature of this approximation space is that the product of two functions in it is also in it: $\hat\psi_1^H \cdot \hat\psi_1^H = \hat\psi_1^H$. Consequently, the matrix of the operation "multiply by $f$,"

$$[f] = \begin{bmatrix}\langle 1|f\rangle & \langle\hat\psi_1^H|f\rangle\\ \langle\hat\psi_1^H|f\rangle & \langle 1|f\rangle\end{bmatrix}, \tag{51}$$

no longer needs any approximation. On the other hand, $\mathcal{L}$ requires some computation. Still, $[\mathcal{L}]$ is diagonal by symmetry

and $\mathcal{L}_{00} = 1$. Also, by straightforward computation with the Legendre generating function,

$$\mathcal{L}_{11} = \langle \hat{\psi}_1^H | \mathcal{L} \hat{\psi}_1^H \rangle = \sum_{n=0}^{\infty} \frac{1}{2(n+1)} \frac{\left| \langle P_n | \hat{\psi}_1^H \rangle \right|^2}{\| P_n \|^2}$$
$$= \frac{3}{4} + \sum_{n \geqslant 1} \frac{4n+3}{n+1} \left( \frac{(2n-1)!!}{(2n+2)!!} \right)^2 \approx 0.83. \quad (52)$$

Then, the ion flux is

$$\langle \hat{\psi}_1^H | J_r \rangle = -J^\star \left[ \overline{G}^2 - \langle \hat{\psi}_1^H | G \rangle^2 \right] \frac{\langle \hat{\psi}_1^H | \varphi_{\rm mxd} \rangle}{B} \quad (53)$$

and the shift of the composite mixed potential is

$$\varphi - \overline{\varphi_{\rm mxd}} = \left[ \langle \hat{\psi}_1^H | G \rangle A - \overline{G} \langle \hat{\psi}_1^H | \Gamma \rangle \mathcal{L}_{11} \right] \frac{\langle \hat{\psi}_1^H | \varphi_{\rm mxd} \rangle}{B}, \quad (54)$$

where

$$A = \overline{G}(J^\star + \overline{\Gamma} \mathcal{L}_{11}),$$
$$B = \overline{G} J^\star + \left( \overline{G\Gamma} - \langle G | \hat{\psi}_1^H \rangle \langle \hat{\psi}_1^H | \Gamma \rangle \right) \mathcal{L}_{11}. \quad (55)$$

Given the current-response characteristics and mixed potentials of the two metals comprising a bimetallic Janus swimmer, Eqs. (53) and (54) could be applied immediately. For example, $\langle \hat{\psi}_1^H | \varphi_{\rm mxd} \rangle$ is just half the mixed potential difference.

The approximations discussed here can be improved by expanding the basis sets; however, it does not seem very practical to attempt that by hand.

## VII. FRUMKIN-BUTLER-VOLMER KINETICS

The purpose of this section is to find expressions for the current-response characteristics $G$ and $\Gamma$ in the framework of FBV kinetics. Frumkin-Butler-Volmer kinetics for the reactions (1) and (2) give the following anodic and cathodic surface fluxes of reactive cation:

$$J_a(\theta) = k_a(\theta) e^{z_r \alpha_a V_s(\theta)/\phi^\star} (C_{\mathcal{R}})^{m_a},$$
$$J_c(\theta) = N k_c(\theta) e^{-N z_r \alpha_c V_s(\theta)/\phi^\star} (C_{\mathcal{R}})^{m_c} \left[ C_r^i(\theta) \right]^N. \quad (56)$$

We assume that reactions are sufficiently slow that heterogeneity of reactant concentration can be neglected, i.e., the Damköhler number is small. The particular case of $z_r \alpha_a = N z_r \alpha_c = \frac{1}{2}$, $N = 1$, and $\cos\theta$ variation of $k_c$ and $k_a$ was considered by Sabass and Seifert [53].

### A. Current-response characteristics

Since the FBV kinetics (56) explicitly requires knowledge of $V_s$ and $C_r^i$, the partitioning of $dV$ into incremental potential drops across the Stern and diffuse layers [see Eq. (6)] must be addressed. The increment equations (32) and (33) need to be followed up with

$$dV_s = f_s dV, \quad (57a)$$
$$dV_d = f_d dV, \quad (57b)$$
$$C_r^i = C_r^o e^{-z_r V_d/\phi^\star}. \quad (57c)$$

The partition coefficients $f_s$ and $f_d$ with $f_s + f_d = 1$ determine the partitioning of the increment of interfacial potential drop into incremental drops across the Stern and diffuse layers. They are inversely proportional to the respective layer capacitances. The capacitance of the diffuse layer is determined by Gouy-Chapman theory, but that of the Stern layer involves specific ion interactions with the surface. A theory to explicitly calculate $f_s$ and $f_d$ is beyond what we do here. These have a similar parametric status as did $G$ and $\Gamma$ in the phenomenological treatment.

Now we can straightforwardly calculate

$$G = z_r N f_d J_c/\phi^\star + f_s z_r (\alpha_a J_a + N \alpha_c J_c)/\phi^\star,$$
$$\Gamma = \frac{1}{2} z_r \phi^\star G + N \frac{Y_r}{C_r^o} J_c. \quad (58)$$

Since the number of FBV parameters involved here is quite large, it is not clear that starting from FBV kinetics is really an advance over the phenomenological parametrization.

### B. Weak heterogeneity

Equation (37) may be used with $G$ and $\Gamma$ as empirical parameters, but we will apply it to a perturbation described in terms of the FBV parameters in (56). We use abbreviations

$$K_a(\theta) := k_a(\theta) e^{z_r \alpha_a V_s(\theta)/\phi^\star},$$
$$K_c(\theta) := k_c(\theta) e^{-N z_r \alpha_c V_s(\theta)/\phi^\star} \quad (59)$$

and for $i = a,c$ decompose $K_i = K_i^0 + \delta K_i$ into uniform metal $K_i^0$ and weak perturbation $\delta K_i$ contributions. Now imagine a uniform metal with mixed potential $\varphi_0$ and uniform kinetic characteristics $K_a^0$ and $K_c^0$, for which the exchange flux is

$$J_{\rm xch}^{(0)} := J_a^{(0)} = J_c^{(0)}. \quad (60)$$

From Eq. (58) we obtain

$$G = g J_{\rm xch}^{(0)}/\phi^\star, \quad \Gamma = (z_r g/2 + h) J_{\rm xch}^{(0)}, \quad (61)$$

where

$$g = z_r N f_d + f_s (z_r \alpha_a + N z_r \alpha_c), \quad h = N \frac{Y_r}{C_r^{o(0)}}. \quad (62)$$

Generally $g$ will be of order 1, while $h$, which measures how salty the solution is, is of order 1 or larger. Then, according to (37),

$$\frac{(\!| J |\!)_m}{J^\star} = \frac{g \left( J_{\rm xch}^{(0)}/J^\star \right)}{1 + [(z_r g + 2h)/2(m+1)] \left( J_{\rm xch}^{(0)}/J^\star \right)} \times \frac{(\!| \overline{\varphi_{\rm mxd}} - \varphi_{\rm mxd} |\!)_m}{\phi^\star} \quad (63)$$

to leading order in the perturbation. To determine $\varphi_{\rm mxd} - \varphi_0$ in terms of the perturbations $\delta K_a$ and $\delta K_c$, imagine them being suddenly switched on. Differentiating (56) shows that a current

$$J_{\rm inst} = \left( \frac{\delta K_a}{K_a^0} - \frac{\delta K_c}{K_c^0} \right) J_{\rm xch}^{(0)}$$

then develops instantaneously. On the other hand, since $G$ gives the bare current response to a potential perturbation,

$$\varphi_{\rm mxd} - \varphi_0 = -\frac{1}{G} J_{\rm inst}$$

to our level of approximation. Therefore, for $m \geqslant 1$,

$$(\!|\overline{\varphi_{\rm mxd}} - \varphi_{\rm mxd}|\!)_m = \frac{J^{(0)}_{\rm xch}}{G}\left(\frac{\delta K_a}{K^0_a} - \frac{\delta K_c}{K^0_c}\right)_m . \qquad (64)$$

For small $C_{\mathcal{R}}$, $J^{(0)}_{\rm xch}$ will be small enough that the denominator of the first factor in (63) is approximately 1 and $J_r$ will share the dependence of $J^{(0)}_{\rm xch}$ on $C_{\mathcal{R}}$. At large enough reactant concentration however, $J_r$ saturates, becoming independent of $C_{\mathcal{R}}$. Note also that saturation happens for smaller $J^{(0)}_{\rm xch}$ in a saltier solution.

## VIII. CONFRONTING EXPERIMENT

The weak-heterogeneity results (63) and (39) exhibit an interesting dependence on swimmer size and fuel concentration. If in Eq. (29) $\Psi(\theta)$ is independent of motor size and fuel concentration (weak heterogeneity is sufficient), then $Ua \propto (\!|J|\!)_m/J^\star$. If we assume that all reactions are first order in fuel concentration $C_{\mathcal{R}}$ and recalling that $J^\star$ in (13) is proportional to $1/a$, then

$$Ua \approx \alpha \frac{C_{\mathcal{R}} a}{\beta + C_{\mathcal{R}} a} \qquad (65)$$

for some parameters $\alpha$ and $\beta$. Sabass and Seifert [53] have previously arrived at a formula with the same structure [Eq. (33) in [53]], working (effectively) under the same assumption of weak inhomogeneity. Since the small-basis results (49) and (53) are structurally very similar to (63), it is plausible that the breakdown of (65) beyond the weak-heterogeneity regime is gradual. A remarkable feature of this scaling form is that it shows that speed saturation at high fuel concentration and speed being inversely proportional to swimmer size are linked phenomena and both are a consequence of the nonlocal feedback effect. The model of Ebbens *et al.* [63] for diffusiophoresis with a two-step reaction chain controlled by the reaction site availability on the surface has the same asymptotic dependence of speed on particle size as in (65): inversely proportional to radius for large particles, independent for small particles. A unifying picture is not evident, but this does show that the size dependence generally does not, *eo ipso*, distinguish mechanisms.

We test the scaling form against the data of Wheat *et al.* [27]. They measured speeds $U$ of spherical Au/Pt bimetallic $H_2O_2$-powered swimmers ($\mathcal{R} = H_2O_2$) with radii of $a = 2$, 3, and 5 $\mu$m over a range of hydrogen peroxide concentrations $C_{H_2O_2}$. The data from their Fig. 4 are replotted as $a\,U$ versus $a\,C_{H_2O_2}$ in Fig. 5. Data collapse is attained well within the error bars: The results are consistent with the scaling form (65). A fit linear in concentration with a radius-dependent slope can be achieved only at the cost of nonzero values at zero concentration [27], which is nonphysical. Within the weak-heterogeneity picture (63) and (64), the fit parameter $\beta$ is related to the $O_2$ evolution rate in a simple way, which should remain qualitatively correct even outside that regime. First, note that $J^\star/2 \approx (3.5 \times 10^{-5}\,\mathrm{mol\,s^{-1}\,m^{-2}})(\mu\mathrm{m}/a)$, using the diffusion coefficient of hydronium and the pH ($\simeq 5.6$) of deionized water equilibrated with atmospheric carbon dioxide. The $O_2$ evolution rate is approximately $J^{(0)}_{\rm xch}/2$, which reaches the value $J^\star/2$ at peroxide concentration $C_{H_2O_2} = \beta/a = 3.13\,\mathrm{M}(\mu\mathrm{m}/a)$. The $O_2$ evolution rate is therefore approximately $(1 \times 10^{-5}\,\mathrm{mol\,s^{-1}\,m^{-2}})(C_{H_2O_2}/M)$ at that specific concentration, but insofar as the evolution rate is proportional to peroxide concentration, this formula remains valid for other $C_{H_2O_2}$. Direct measurement (see footnote 20 in Ref. [64]) for Pt/Au nanorods (370 nm diameter, 2 $\mu$m length) in 3.7% $H_2O_2$ shows the $O_2$ evolution rate is about $(0.8 \times 10^{-5}\,\mathrm{mol\,s^{-1}\,m^{-2}})(C_{H_2O_2}/M)$, in remarkably close agreement with our estimate based on a fitting parameter for swimmer speed.

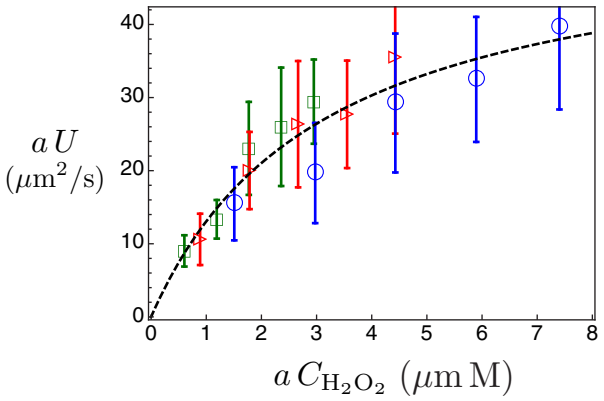


FIG. 5. (Color online) Scaling collapse. Data of Wheat *et al.* [27] for $H_2O_2$-powered bimetallic spherical swimmers of radii 2 $\mu$m (□), 3 $\mu$m (▷), and 5 $\mu$m (◯) are plotted in the scaling form (65). The fit parameters are $\alpha = 54.0\ \mu\mathrm{m}^2/\mathrm{s}$ and $\beta = 3.13\ \mu$m M, with a reduced $\chi^2$ of 0.22.

The scaling form (65) is independent of the order of the kinetics in anything except fuel concentration. For an analogous fit assuming second-order kinetics in $C_{\mathcal{R}}$, we find a reduced $\chi^2$ goodness-of-fit measure of 0.37, significantly worse than the score (0.22) for the first-order fit. The total oxygen evolution rate can also be deduced in this case and is more than an order of magnitude larger than the result from the first-order fit.

## IX. CONCLUSION

The "transmissions" of electrocatalytic motors (i.e., phoretic phenomena immediately linked to the motion) have received considerably more theoretical attention than the underlying "engines". Self-consistent nonlocal feedback theory presents a flexible general framework for considering the heterogeneous electrochemical problem posed by the "engine," which is based on the idea of using an imaginary bias field as control parameter. The method interfaces neatly both with fundamental Frumkin-Butler-Volmer kinetics and with operational laboratory concepts. Previous results are obtained as the simplest approximation. As a first fruit of this approach, a scaling form for swimmer speed has been found that seems to have been previously unsuspected. We hope that more complete experimental data on electrochemical response will soon make more rigorous tests possible.

## ACKNOWLEDGMENTS

This work was supported by the National Science Foundation under Grant No. DMR-1420620 through the Penn State Center for Nanoscale Science. We thank Tom Mallouk for reading the manuscript and giving a chemist's opinion.

[1] W. Wang, W. Duan, S. Ahmed, T. E. Mallouk, and A. Sen, Nano Today **8**, 531 (2013).
[2] G. A. Ozin, ChemCatChem **5**, 2798 (2013).
[3] W. Gao and J. Wang, ACS Nano **8**, 3170 (2014).
[4] S. Sengupta, M. E. Ibele, and A. Sen, Angew. Chem. Int. Ed. Engl. **51**, 8434 (2012).
[5] T. Mirkovic, N. S. Zacharia, G. D. Scholes, and G. A. Ozin, Small **6**, 159 (2010).
[6] S. J. Ebbens and J. R. Howse, Soft Matter **6**, 726 (2010).
[7] J. Wang and K. M. Manesh, Small **6**, 338 (2010).
[8] T. Mirkovic, N. S. Zacharia, G. D. Scholes, and G. A. Ozin, ACS Nano **4**, 1782 (2010).
[9] J. Wang, ACS Nano **3**, 4 (2009).
[10] W. F. Paxton, S. Sundararajan, T. E. Mallouk, and A. Sen, Angew. Chem. Int. Ed. Engl. **45**, 5420 (2006).
[11] H. H. Kung and M. C. Kung, Appl. Catal. A **309**, 159 (2006).
[12] R. Dreyfus, J. Baudry, M. L. Roper, M. Fermigier, H. A. Stone, and J. Bibette, Nature (London) **437**, 862 (2005).
[13] W. Paxton, A. Sen, and T. Mallouk, Chem. Eur. J. **11**, 6462 (2005).
[14] G. Ozin, I. Manners, S. Fournier-Bidoz, and A. Arsenault, Adv. Mater. **17**, 3011 (2005).
[15] A. Nourhani, V. H. Crespi, and P. E. Lammert, Phys. Rev. E **90**, 062304 (2014).
[16] R. Golestanian, T. B. Liverpool, and A. Ajdari, New J. Phys. **9**, 126 (2007), .
[17] E. Purcell, Am. J. Phys. **45**, 3 (1977).
[18] P. Colinvaux, Nature (London) **277**, 353 (1979).
[19] M. G. L. van den Heuvel and C. Dekker, Science **317**, 333 (2000).
[20] M. Schliwa and G. Woehlke, Nature (London) **422**, 759 (2003).
[21] C. Mavroidis, A. Dubey, and M. L. Yarmush, Annu. Rev. Biomed. Eng. **6**, 363 (2004).
[22] W. Paxton, K. Kistler, C. Olmeda, A. Sen, S. S. Angelo, Y. Cao, T. Mallouk, P. Lammert, and V. Crespi, J. Am. Chem. Soc. **126**, 13424 (2004).
[23] P. Dhar, T. M. Fischer, Y. Wang, T. E. Mallouk, W. F. Paxton, and A. Sen, Nano Lett. **6**, 66 (2006).
[24] R. Laocharoensuk, J. Burdick, and J. Wang, ACS Nano **2**, 1069 (2008).
[25] U. K. Demirok, R. Laocharoensuk, K. M. Manesh, and J. Wang, Angew. Chem. Int. Ed. Engl. **47**, 9349 (2008).
[26] N. S. Zacharia, Z. S. Sadeq, and G. A. Ozin, Chem. Commun. **39**, 5856 (2009).
[27] P. M. Wheat, N. A. Marine, J. L. Moran, and J. D. Posner, Langmuir **26**, 13052 (2010).
[28] A. Nourhani, P. E. Lammert, A. Borhan, and V. H. Crespi, Phys. Rev. E **87**, 050301(R) (2013).
[29] A. Nourhani, Y.-M. Byun, P. E. Lammert, A. Borhan, and V. H. Crespi, Phys. Rev. E **88**, 062317 (2013).
[30] S. Fournier-Bidoz, A. C. Arsenault, I. Manners, and G. A. Ozin, Chem. Commun. **4**, 441 (2005).
[31] L. Qin, M. J. Banholzer, X. Xu, L. Huang, and C. A. Mirkin, J. Am. Chem. Soc. **129**, 14870 (2007).
[32] Y. Wang, S.-t. Fei, Y.-M. Byun, P. E. Lammert, V. H. Crespi, A. Sen, and T. E. Mallouk, J. Am. Chem. Soc. **131**, 9926 (2009).
[33] J. G. Gibbs, S. Kothari, D. Saintillan, and Y. P. Zhao, Nano Lett. **11**, 2543 (2011).
[34] J. G. Gibbs and Y. Zhao, Small **6**, 1656 (2010).
[35] J. G. Gibbs and Y.-P. Zhao, Small **5**, 2304 (2009).
[36] L. F. Valadares, Y.-G. Tao, N. S. Zacharia, V. Kitaev, F. Galembeck, R. Kapral, and G. A. Ozin, Small **6**, 565 (2010).
[37] T. R. Kline, W. F. Paxton, T. E. Mallouk, and A. Sen, Angew. Chem. Int. Ed. Engl. **44**, 744 (2005).
[38] J. Burdick, R. Laocharoensuk, P. M. Wheat, J. D. Posner, and J. Wang, J. Am. Chem. Soc. **130**, 8164 (2008).
[39] P. Calvo-Marzal, K. M. Manesh, D. Kagan, S. Balasubramanian, M. Cardona, G.-U. Flechsig, J. Posner, and J. Wang, Chem. Commun. **30**, 4509 (2009).
[40] J. L. Anderson, Annu. Rev. Fluid Mech. **21**, 61 (1989).
[41] D. A. Saville, Annu. Rev. Fluid Mech. **9**, 321 (1977).
[42] R. A. Rica and M. Z. Bazant, Phys. Fluids **22**, 112109 (2010).
[43] E. Yariv, J. Fluid Mech. **655**, 105 (2010).
[44] E. Yariv, Proc. R. Soc. London Ser. A **465**, 709 (2009).
[45] O. Schnitzer and E. Yariv, Phys. Rev. E **86**, 061506 (2012).
[46] Y. Ben, E. A. Demekhin, and H.-C. Chang, J. Colloid Interface Sci. **276**, 483 (2004).
[47] B. Zaltzman and I. Rubinstein, J. Fluid Mech. **579**, 173 (2007).
[48] A. Nourhani, P. E. Lammert, V. H. Crespi, and A. Borhan, Phys. Fluids **27**, 012001 (2015).
[49] J. L. Moran, P. M. Wheat, and J. D. Posner, Phys. Rev. E **81**, 065302 (2010).
[50] W. Wang, T.-Y. Chiang, D. Velegol, and T. E. Mallouk, J. Am. Chem. Soc. **135**, 10557 (2013).
[51] E. Yariv, Proc. R. Soc. London Ser. A **467**, 1645 (2011).
[52] J. L. Moran and J. D. Posner, J. Fluid Mech. **680**, 31 (2011).
[53] B. Sabass and U. Seifert, J. Chem. Phys. **136**, 214507 (2012).
[54] E. Yariv, Chem. Eng. Commun. **197**, 3 (2010).
[55] I. Bikri, R. B. Guenther, and E. A. Thomann, Discrete Contin. Dyn. Syst. Ser. S **3**, 221 (2010).
[56] M. E. Taylor, *Partial Differential Equations II. Qualitative Studies of Linear Equations*, 2nd ed., Applied Mathematical Sciences Vol. 116 (Springer, New York, 2011), pp. xxii and 614.
[57] B. N. Khoromskij and G. Wittum, *Numerical Solution of Elliptic Differential Equations by Reduction to the Interface*, Lecture Notes in Computational Science and Engineering Vol. 36 (Springer, Berlin, 2004), pp. xii and 293.
[58] P. M. Morse and H. Feshbach, *Methods of Theoretical Physics* (McGraw-Hill, New York, 1953), Vol. 1, pp. xxii, 1–997, and xl; Vol. 2, pp. xviii and 999–1978.
[59] J. D. Jackson, *Classical Electrodynamics*, 2nd ed. (Wiley, New York, 1975), pp. xxii and 848.
[60] J. L. Anderson and D. C. Prieve, Langmuir **7**, 403 (1991).
[61] D. C. Prieve, J. L. Anderson, J. P. Ebel, and M. E. Lowell, J. Fluid Mech. **148**, 247 (1984).
[62] Y. Wang, R. M. Hernandez, D. J. Bartlett, J. M. Bingham, T. R. Kline, A. Sen, and T. E. Mallouk, Langmuir **22**, 10451 (2006).
[63] S. Ebbens, M.-H. Tu, J. R. Howse, and R. Golestanian, Phys. Rev. E **85**, 020401 (2012).
[64] W. F. Paxton, P. T. Baker, T. R. Kline, Y. Wang, T. E. Mallouk, and A. Sen, J. Am. Chem. Soc. **128**, 14881 (2006).